Mechanical Systems and Signal Processing 153 (2021) 107499

Contents lists available at ScienceDirect

Mechanical Systems and Signal Processing

journal homepage: www.elsevier.com/locate/ymssp

Obstruction-invariant occupant localization using footstep-induced structural vibrations

Mostafa Mirshekari [a,*], Jonathon Fagert [a], Shijia Pan [c], Pei Zhang [b], Hae Young Noh [a]

[a] Civil and Environmental Engineering, Carnegie Mellon University, Pittsburgh, PA 15213, USA
[b] Electrical and Computer Engineering, Carnegie Mellon University, Moffett Field, CA 94035, USA
[c] Department of Computer Science and Engineering, University of California, Merced, CA 95343, USA

ARTICLE INFO

Article history:
Received 23 December 2019
Received in revised form 13 September 2020
Accepted 26 November 2020
Available online 28 December 2020

Keywords:
Structural vibrations
Occupant localization
Obstruction
Structural vibration
Non-isotropic multilateration

ABSTRACT

In this paper, we characterize the effects of obstructions on footstep-induced floor vibrations to enable obstruction-invariant indoor occupant localization. Occupant localization is important in smart building applications such as smart healthcare and energy management. Maintenance and installment requirements limit the application of current sensing approaches (e.g., mobile-based, RF-based, and pressure-based sensing) in real-life applications. To overcome these limitations, prior work has utilized footstep-induced structural vibrations for occupant localization. The main intuition behind these approaches is that the footstep-induced floor vibration waves take different amounts of time to arrive at different sensors. These Time-Differences-of-Arrival (TDoA) can then be leveraged to locate the footstep by assuming similar velocities between the footstep and various sensor locations. This assumption makes these approaches suitable for open areas; however, real buildings have various types of obstructions (e.g., walls, furniture, etc.) which affect wave propagation velocities and hence significantly reduce localization accuracy. Therefore, the prior work requires unobstructed paths between footsteps and sensors for accurate occupant localization, which increases the sensing density requirement and thus, instrumentation and maintenance costs. We have observed that the obstruction mass is one of the key factors in affecting the wave propagation velocity and reducing the localization accuracy. Therefore, to overcome the obstruction challenge, we localize footsteps by considering different velocities between the footsteps and sensors depending on the existence and mass of obstruction on the wave path. Specifically, we (1) detect and estimate the mass of the obstruction by characterizing the wave attenuation rate, (2) use this estimated mass to find the propagation velocities for localization by modeling the velocity-mass relationship through the lamb wave characteristics, and (3) introduce a non-isotropic multilateration approach which robustly leverages these propagation velocities to locate the footsteps (and the occupants). In field experiments, we achieved average localization error of 0.61 meters, which is (1) the same as the average localization error when there is no obstruction and (2) 1.6X improvement compared to the baseline approach.

* Corresponding author.
E-mail addresses: mmirshekari@cmu.edu (M. Mirshekari), jfagert@cmu.edu (J. Fagert), span24@ucmerced.edu (S. Pan), peizhang@cmu.edu (P. Zhang), noh@cmu.edu (H.Y. Noh).

https://doi.org/10.1016/j.ymssp.2020.107499
0888-3270/

1. Introduction

Step-level occupant localization is useful in various smart building applications such as senior/healthcare and energy management. For example, knowing the footstep location enables non-intrusive patient monitoring in common residential and commercial buildings through estimating gait-related features such as stride length and walking speed. This allows timely diagnosis and treatment of diseases such as dementia, chronic obstructive pulmonary disease, and muscular dystrophy [1–5]. Further, knowing the location of the occupants inside the building enables efficient heating and cooling which ensures the comfort of the occupants while reducing the energy consumption [6–8]. Some of the current sensing approaches for occupant localization include mobile-based [9–12], Radio-Frequency-based (RF) [13–15], and pressure-based [16–18] approaches. However, the application of these approaches in real-life scenarios is limited due to installment and maintenance requirements. Mobile-based approaches require the occupants to carry or wear a device which might be difficult to enforce in some applications (e.g., senior/healthcare) [9–12]. On the other hand, RF-based and pressure-based sensing either require dense sensor deployment or extensive calibration for step-level occupant localization [13–18].

To overcome these limitations, prior work has explored non-intrusive human footstep location estimation using structural vibrations [19]. The intuition is that footsteps induce floor vibrations, which propagate through the floor structure to multiple sensors and arrive at different sensors at different times. These Time Differences of Arrival (TDoA) of waves between various sensor pairs are used to localize the occupants through multilateration approach. This approach assumes that the wave propagation velocities between the footstep and the sensors are similar (i.e., isotropic behaviour) and therefore, is suitable for open spaces. However, in real life structures, there are various types of obstruction (e.g., walls, furniture, etc.) which affect the floor structural properties and hence the wave propagation velocity [20]. In turn, these changes in propagation velocity can significantly reduce the occupant localization accuracy. Therefore, to maintain the localization accuracy, the prior works require multiple sensors with unobstructed wave propagation path to footsteps in every room which increases the instrumentation and maintenance costs [19,21–24].

In this paper, we introduce an obstruction-invariant footstep-vibration-based occupant localization approach which considers different wave propagation velocities between the footstep and various sensors depending on the existence and the mass of the obstruction. By considering the obstruction effect, we improve the localization performance of the vibration-based sensing in obstructive indoor settings while reducing the instrumentation and maintenance requirements. To achieve this goal, the main research challenges are that (1) the relationship between the wave propagation velocity and the obstruction mass is unknown and structure-dependent and (2) for each footstep, the existence and the mass of obstruction on the vibration wave path is also unknown. To overcome these challenges, we first characterize the frequency-dependent attenuation of the footstep-induced vibrations to find the existence and mass of the obstruction on the path between the footstep and each sensor using the signal energy. Then, we employ the lamb wave propagation characteristics to model the velocity-mass relationship which is suitable for various structures. This relationship enables finding the wave propagation velocities between the footstep and the sensors. Finally, we introduce a non-isotropic and grid-search-based multilateration approach which estimates the footstep location when the propagation velocities between the footstep and different sensors are different. The objective of this paper is to design a novel, practical, and end-to-end sensing approach for occupant localization in obstructive indoor settings. To validate the system performance, we use field experiments in multiple structure with human participants.

In summary, the core contributions of this paper are:

- We present a step-level occupant localization approach which is robust to the existence of obstructions (e.g., furniture and walls) using footstep-induced floor vibration.
- We employ physical principles of lamb wave propagation to characterize the effects of the obstruction mass on the wave attenuation rate and propagation velocity. This characterization enables estimating the existence and mass of the obstruction and in turn, the footstep-sensor wave propagation velocities for new footsteps. Finally, we leverage these velocities to locate the occupants using our non-isotropic multilateration approach.
- We evaluate the step-level occupant localization when there exists an obstruction in various structures with different structural materials and characteristics.

The rest of the paper is organized as follows: First, we discuss the related works and how our work is distinguished from them (in Section 2). Then, we discuss the physical intuition behind lamb wave propagation characteristics and how it is affected by the addition of an obstruction mass (in Section 3). Next, we discuss our obstruction-invariant occupant localization approach (in Section 4). Finally, we describe our evaluation procedure, including the experiments we conducted and the analysis results (in Section 5), and conclude our work.

2. Related work

In this section, we explore the related work and the remaining research gap for different aspects of vibration-based occupant localization in obstructed indoor settings. We first discuss the existing approaches for analyzing the addition of mass on the floor. Then, we describe the general source localization and the vibration-based occupant localization approaches.

2.1. Mass addition for wave propagation and structural vibration control

Existence of mass on the floor affects the structural dynamic properties as well as the vibration wave propagation characteristics. Based on this effect, adding a series of masses (and mass dampers) in designated locations on the floor have been used to control the structural vibrations and noise of the floors [25–28]. The main goal of this process is to modify the modal characteristics of the floor to attenuate the vibration noise and improve the living condition for the residents. Further, the effect of mass on wave propagation velocity has been studied for guiding and focusing flexural lamb waves via adding elastic metamaterial masses [29,30]. However, these approaches are not suitable in our problem. First, they are focused on the forward problem of how the addition of mass affects the structural vibrations, whereas our problem is an inverse problem (i.e., finding mass based on the structural vibration). Second, they develop a physical model which is difficult in real-life floors for which the structural parameters and configuration are often unknown and uncertain. To overcome these limitations, we introduce a physics-guided, data-driven approach to (1) estimate the obstruction mass using the structural vibration and (2) characterize the relationship between the obstruction mass and wave propagation velocity.

2.2. Floor-vibration-based occupant localization

The objective of the floor-vibration-based occupant localization is to estimate the unknown footstep location using the vibration signals received in multiple sensors of known location. This field of study is a building-scale version of vibration source localization, which is common in the field of earthquake engineering and seismology [31–33]. The main current approaches for occupant localization include classification-based approaches, TDoA-based approaches, and physical-model-based approaches. The classification approach aims to match the signals received in various locations to a set of signals from known locations [34]. TDoA-based approaches leverage the fact that the vibration waves caused by the footsteps arrive at different sensors at different times. A common approach to leverage these TDoAs is multilateration [19,22–24]. Multilateration is based on the fact that the possible locations of the footstep given a specific Time Difference of Arrival (TDoA) between two sensors and wave propagation velocity form a hyperbola. Having more sensors results in additional TDoAs and hyperbolas whose intersection is the footstep location. Alternatively, the sign of the TDoAs can be used to locate the footstep by recurrent division of the search space [35].

However, obstructions such as walls and furniture affect the wave propagation characteristics. This effect results in either extensive calibration requirements, higher sensing requirements, or reduced localization performance for the classification-based and TDoA-based approaches. The physical-model-based approaches compare the vibration measurements with the physical model predictions to estimate the occupant location. Hence, they potentially can handle the obstruction effect by including it in the physical model [6,36]. However, these approaches require knowing the structural characteristics for modeling which might not be known in many buildings. In this paper, based on lamb wave properties, we characterize the relationship between the wave propagation velocity and the obstruction mass to enable TDoA-based occupant localization. This approach does not require extensive calibration or knowing the structural characteristics.

3. The physics behind obstruction effect on footstep-induced vibration wave propagation

We utilize the footstep-induced floor vibrations to localize the occupants in obstructive indoor settings. In this section, we provide a brief background of the physics of the footstep-induced floor vibration wave propagation and how it is affected by obstructions such as walls and furniture. The footsteps cause elastic vibration waves in the floor which travels outward from the footstep location. These elastic vibration waves can be formulated as Lamb waves because (1) the floors are plates with free surfaces on the top and bottom and (2) due to the low frequency nature of the footstep vibrations, the ratio of wavelength to floor thickness is large in our application [37,19].

The Effect of Obstruction Mass on the Lamb Wave Attenuation Rate: The attenuation rate of the Lamb waves depends on the floor mass and the frequency (i.e., higher frequency components show higher attenuation rate) [38]. The addition of the obstruction results in larger mass which in turn results in additional frequency-dependent attenuation. In other words, obstructions cause different levels of energy reduction across various frequency components of the vibration wave. For a specific component, this attenuation can potentially be used to estimate the obstruction mass by modeling the relationship between the obstruction mass and the component energies. However, these component energies also depend on the footstep force and thus, it is difficult to find out if the energy reduction is caused by the addition of the mass or a lighter footstep. To negate the effect of the footstep force, we instead model the relationship between the obstruction mass and the ratios of the different frequency component amplitudes. The main intuitions are: (1) the obstruction-induced wave attenuation rate is frequency-dependent and (2) for the small displacements caused by the footsteps, the structure behaves linearly and hence increasing the footstep force results in a similar increase in all the frequency component amplitudes (e.g., if the footstep force is twice as large, the amplitude of all the frequency components is approximately twice as large). Therefore, by considering the frequency amplitude ratios, we keep the effect of the obstruction while negating the effect of the footstep force. Fig. 1 shows the changes in a sample ratio for different mass levels (ratio of frequency amplitude at 10 Hz over the amplitude at 60 Hz). These specific frequencies are chosen empirically for better illustration of the obstruction effect intuition. This figure shows that

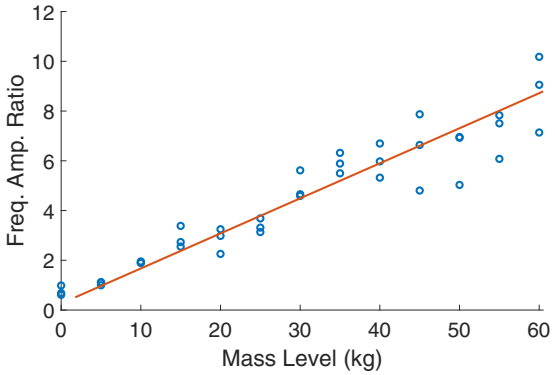

Fig. 1. The Effect of the Obstruction Mass on the Frequency Amplitude Ratios (ratio of frequency amplitude at 10 Hz over the amplitude at 60 Hz). This figure shows that addition of the mass results in higher ratio between the amplitude of these components which means that the attenuation at 60 Hz is more significant than the attenuation at 10 Hz.

addition of the mass results in higher ratio which means that the attenuation at 60 Hz is more significant than the attenuation at 10 Hz.

The Effect of Obstruction Mass on Lamb Wave Propagation Velocity: In general, Lamb waves show two infinite sets of propagation modes: symmetric (S) and anti-symmetric (A). However, for low frequency footstep-induced vibrations, only the zeroth order modes (i.e., S_0 and A_0) can exist and among them, the A_0 modes are most pronounced in magnitude (while S_0 modes are barely visible and hence negligible) [39]. For asymmetrical modes of low frequency (i.e., long flexural waves), the wave propagation velocity is estimated using [40]

$$V^2 = \frac{4}{3}\xi^2 f^2 \frac{\lambda+\mu}{\lambda+2\mu}\frac{\mu}{\rho} \tag{1}$$

where μ and λ are the Lamé constants which describe the material properties, $2f$ is the thickness of the plate, ξ is the wavenumber, and ρ is the material density. This equation is based on the assumption of an infinite plate. One of the main differences between a finite and infinite medium is the reflection and refraction effect which happens in the finite medium. However, for localization purposes, the most important part of the vibration wave signal is the first arrival, which happens in the shortest path (with no reflection). This first arrival is used for estimating the Time-Difference-of-Arrival (TDoA) between sensors which is then mapped to the footstep location. Further, from our experiments, the waves dissipate between footsteps, thus each footstep can be assessed independently. Therefore, the assumption of an infinite plate is a reasonable approximation for our localization problem. Based on this equation, for given floor thickness and material properties, the wave propagation velocity depends on (1) the floor mass which can be affected by the obstruction mass and (2) the frequency (i.e., is dispersive). We use these two principles in designing our obstruction-invariant occupant localization approach, as will be discussed in Section 4.2. Fig. 2 shows that adding more mass results in lower wave propagation velocity. This is shown by reduced ratio of the obstructed velocity to the unobstructed velocity (which does not change across mass levels).

Fig. 3 shows an intuitive illustration of the effects of the obstruction on the wave propagation attenuation and velocity. This figure shows the footstep caused by an occupant walking and two sensors of the same distance to the footstep. To reach

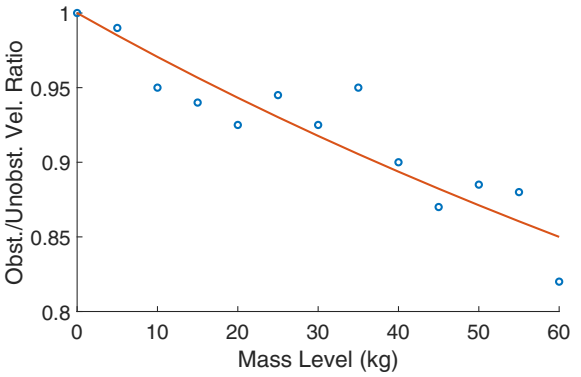

Fig. 2. The effect of the obstruction mass on the wave propagation velocity. This figure shows that adding more mass results in lower wave propagation velocity.

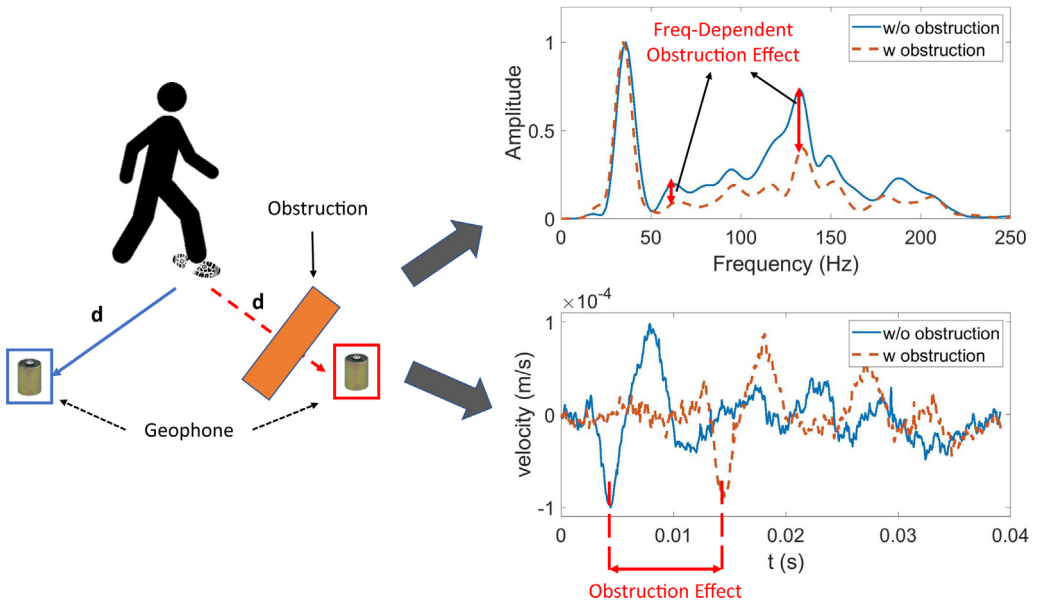

Fig. 3. The obstruction effect intuition. The obstruction affect the signals in both time and frequency domain. These observations are the cornerstone of our obstruction-invariant occupant localization approach.

one of these sensors, the footstep-induced vibration wave propagates through an obstruction. The frequency domain representations of the vibration signals show the frequency-dependent nature of obstruction-induced attenuation. For example, the frequency component of 140 Hz has higher attenuation than the component of 60 Hz. In this figure, we have normalized both signals to have the same maximum to reduce the differences caused by footstep force. On the other hand, the time domain representations of the signals show that the vibration waves reach the obstructed sensor later than the unobstructed sensor. Considering the same footstep-sensor distance, we can conclude that the wave propagation velocity is lower for the obstructed case. This observation is in line with the lamb wave propagation characteristics mentioned in Eq. (1). These observations and principles form the cornerstone of our obstruction-invariant occupant localization approach which is discussed in Section 4.

4. Obstruction-invariant occupant localization

Our approach improves robustness to obstructions by accounting for velocity differences when obstructions of different mass are present. To this end, the approach consists of three main modules: (1) footstep detection, (2) obstruction characterization, and (3) step-level localization. The different stages of this approach are presented in Fig. 4.

4.1. Footstep detection module

The footstep detection module collects the floor vibration data and then extracts the parts of signal that correspond to footstep-induced floor vibration responses. Data collection is performed using geophones which are low cost vibration sensors that measure the vertical velocity of floor vibration [41]. Then, the vibration signals are amplified using an op-amp to improve their resolution [42]. Finally, the signals are digitized and transferred to PC for further analysis. An example of our sensing system is presented in Fig. 5.

The ambient vibration signal sensed by our system consists of impulsive vibration events (such as footsteps, object falls, and door closings) and periodic or white background noise (such as machinery or measurement noise). To ensure we are localizing footsteps and not the other irrelevant impulsive events, we extract the footsteps from a mixture of possible impulsive excitations. To this end, we first detect any impulsive excitations using a variance-based anomaly detection method and then distinguish between footsteps and other impulses using a model-transfer-based SVM classifier [43,44].

The variance-based anomaly detection approach finds the parts of the signal which are of higher variance compared to the ambient noise. To this end, we consider a sliding window over the signal and for each window evaluate the null hypothesis $H_0 : \sigma_w^2 = \sigma_n^2$ (i.e., the windowed signal is noise) against the alternative hypothesis $H_1 : \sigma_w^2 \neq \sigma_n^2$. In these equations, σ_w^2 is the variance of the windowed signal and σ_n^2 is the variance of the ambient noise which is found based on a part of signal with no impulsive vibration event. This test is a Chi-squared test because the variance of a Gaussian ambient noise follows a scaled Chi-squared distribution. The signal windows for which the null hypothesis is rejected are detected as impulsive excitations [19]. The model-transfer-based SVM classifier aims to train a footstep model which distinguishes the footsteps from

other impulsive excitations across different structures. To this end, we first project the data into a space in which the structural effects are minimized and therefore, the data mainly represents the excitations. Then, we train a SVM classifier in the projected space [43,45,44]. Fig. 5 shows an example of the impulse detection process.

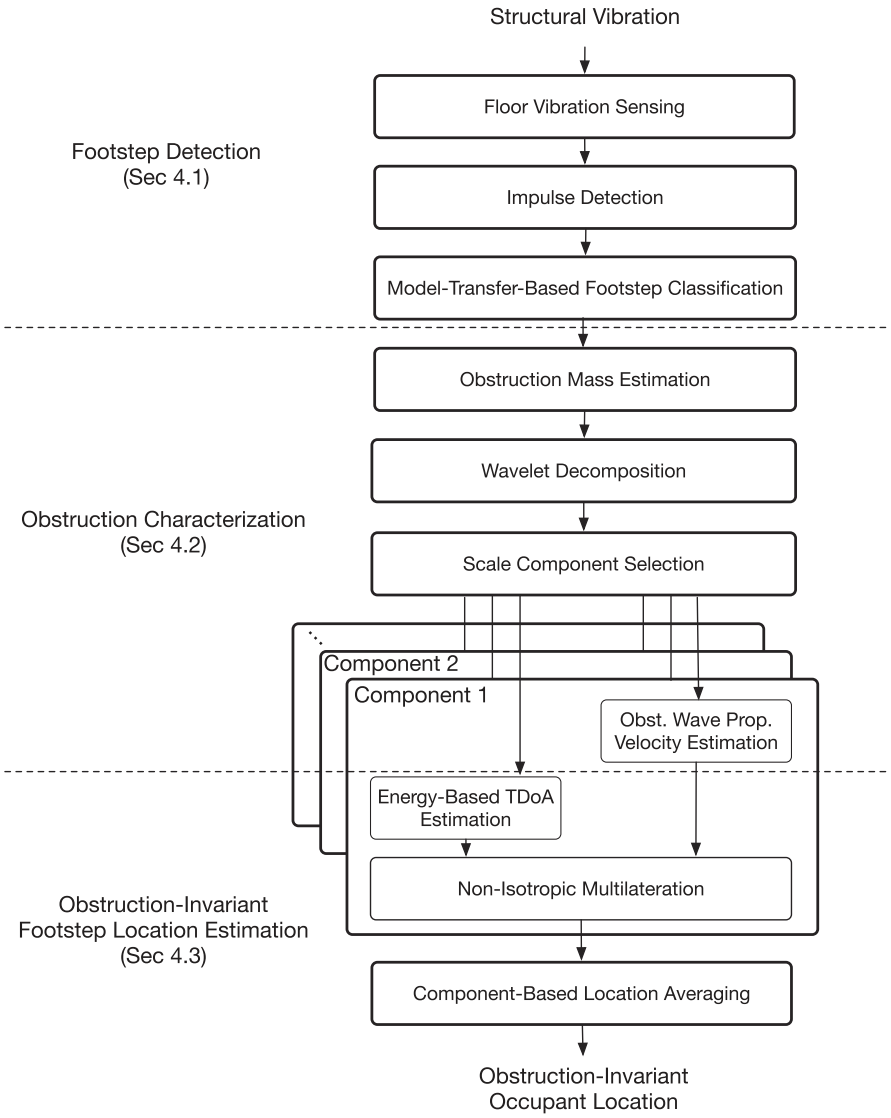

Fig. 4. Obstruction-invariant occupant localization approach.

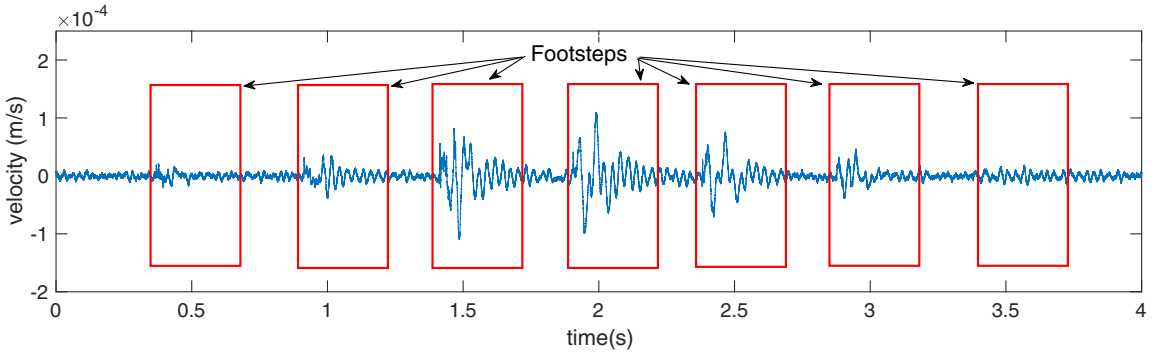

Fig. 5. An example of footstep-induced floor vibration signals measured by a geophone.

4.2. Obstruction characterization module

Our obstruction characterization module first detects and estimates the obstruction mass and then finds the wave propagation velocities when the wave propagates through the obstruction.

Based on the lamb wave propagation characteristics, this propagation velocity is frequency-dependent (aka, the dispersion effect [22,19]) and depends on the obstruction mass, as discussed in Section 3. Therefore, we first decompose the signal into scale components using a time frequency representation and select a subset of scale components with high energy in all the sensors. Then, for each chosen scale component, we estimate the wave propagation velocity knowing the obstruction mass.

4.2.1. Obstruction mass estimation

To detect and estimate the obstruction mass, we characterize the wave attenuation rates caused by the obstruction. Based on the discussion in Section 3, we characterize the relationship between the obstruction mass and the ratios of the amplitude of various frequency components (which are estimated using fft [46]). Further, for the small displacements caused by the footsteps, the structure behaves linearly and thus, we assume a linear relationship between the frequency amplitude ratios and the mass levels. However, considering the ratios between various frequency components results in a large number of ratio features which in turn increase the chance of model over-fitting. Therefore, we first choose a subset of the ratios for training a mass-ratio model. To this end, we first divide the footstep vibration data into training, validation, and test sets. Then, using the training data, we choose a subset of the ratios which have (1) low standard deviation across the samples in the training set (to improve the robustness) and (2) large correlation coefficient with the mass levels (to ensure the linearity and improve accuracy). Then, among the chosen ratios, we employ a greedy wrapper approach to select the ratio features which result in lower validation error [47]. These remaining feature are then used for training a linear model which is used for detecting and predicting the obstruction mass using the footstep-induced vibration events in the test set. This model is trained for the footsteps that happen in a specific location (e.g., the entrance of the apartment in real-life applications).

4.2.2. Wavelet decomposition

To characterize the dispersive (i.e., frequency-dependent) wave propagation velocities, we have decomposed the signal using the wavelet transform which is suitable for analyzing and decomposing non-stationary signals (e.g., impulsive signals such as footsteps) [19,48]. The wavelet decomposition can be described as [49],

$$T(a,b) = w(a)\int_{-\infty}^{+\infty} x(s)\Psi_{b,a}^{*}(s)ds \tag{2}$$

in which $w(a)$ is a weighting function and $\Psi_{b,a}(s)$ is the dilated and time-shifted version of the basis function which is called the mother wavelet $\Psi(s)$. In this paper, we have chosen the Mexican hat wavelet as the mother wavelet because it provides a good representation of the footstep-induced vibration signal characteristics [50]. To select the range of the scales to be analyzed, we have used two notions: (1) geophones are second-degree high pass filters for frequencies lower than 10 Hz [51] and (2) the bandwidth of geophone is 240 Hz [41]. Therefore, the range of the scales we have used for this analysis is between 25 and 300 (i.e., approximately 20 and 250 Hz for sampling rate of 25.6 kHz and Mexican hat wavelet).

4.2.3. Scale component selection

Using all the scale components for localization is not suitable because (1) it is computationally expensive and (2) it decreases the localization performance because the obstruction-induced attenuation potentially causes low-energy scale components with low Signal-to-Noise-Ratio (SNR) which result in large localization errors. Therefore, to overcome the additional obstruction-induced attenuation, we choose a subset of the scale components with high energies in all the sensors for localization. Specifically, we first average the scale component energies across the sensors and then choose the n components with the highest average energy. Choosing the n is an important part of this process. On the one hand, choosing higher n results in reduced effect of noise and outliers. On the other hand, choosing scales of low energy results in large errors in location estimation. This trade-off will be discussed in more detail in Section 5.4.2. In this paper, we have empirically chosen $n = 2$.

4.2.4. Obstructed wave propagation velocity estimation

We estimate the propagation velocity of the vibration wave travelling through an obstruction based on Lamb wave propagation characteristics. Specifically, based on Eq. (1), we estimate the obstructed velocity as the ratio of the unobstructed velocity for a given scale (or frequency) component through

$$\frac{V_{obs}^2}{V_{unobs}^2} = \frac{\frac{4}{3}\xi^2 f \frac{\lambda+\mu}{\lambda+2\mu}\frac{\mu}{\rho_a+m_{obs}}}{\frac{4}{3}\xi^2 f \frac{\lambda+\mu}{\lambda+2\mu}\frac{\mu}{\rho_a}} \tag{3}$$

where μ and λ are the Lamé constants which describe the material properties, $2f$ is the thickness of the plate, ξ is the wavenumber, ρ_a is the mass of the floor per unit of area, m_{obs} is the mass of the obstruction, and V_{obs} and V_{unobs} are the obstructed and unobstructed velocities. We can simplify this equation because (1) we use specific decomposed scale com-

ponents and hence the wavenumber is constant, (2) the Lamé constants depend on the Poisson ratio and the modulus of elasticity, which are a function of the structural material and therefore do not change with obstruction, and (3) we assume that the obstruction does not affect the effective thickness of the floor because it simply sits on the floor or has minimal connection to the floor and hence, there is no significant structural integrity (which is true for most common obstructions such as furniture and non-load-bearing partition walls). Therefore, we have

$$\frac{V_{obs}}{V_{unobs}} = \sqrt{\frac{\rho_a}{\rho_a + m_{obs}}}. \tag{4}$$

Using Eq. (4), we estimate the obstructed velocity based on the unobstructed wave propagation velocity, the mass of obstruction, and the mass per unit of area of the floor. The unobstructed velocity can be estimated either using additional unobstructed sensors or during the time that the obstruction is not present (through either calibration or our prior calibration-free approach [19]). The obstruction mass was estimated in Section 4.2.1. Finally, the floor mass can be estimated using the specification sheets and the available structural drawings.

4.3. Obstruction-invariant footstep location estimation module

This module performs step-level and obstruction-invariant occupant localization using our non-isotropic multilateration approach which considers different wave propagation velocities between the footsteps and sensors based on the obstruction mass on the wave path. To this end, we first estimate the Time of Arrivals (ToA) for the vibration signals using an energy-based approach. Then, we utilize these ToAs and the propagation velocities (estimated in Section 4.2.4) for step-level localization through a non-isotropic multilateration approach. We perform this location estimation for the scale components selected in Section 4.2.3 and combine their estimations to find the step-level occupant location.

4.3.1. Energy-based TDoA estimation

To find the TDoA between the signals, we have estimated the time where a certain percentage of the energy of footstep-induced vibration happens for each sensor. Generally, current approaches for estimating the TDoA are either threshold-based [19,52] or similarity-based (e.g., cross-correlation) [53]. This energy-based approach is more robust than the current approaches because it is less affected by (1) missing peaks compared to the peak-based approaches and (2) signal distortions caused by reflections, dispersion, and multipath compared to the similarity-based approaches [54]. We have observed that considering the transient part of the vibration signals for finding the TDoAs result in more accurate estimations. With that in mind, too small of a value for this threshold results in finding the TDoA using the noisy part of the signal and too large of a value results in missing the arrival time of the signals. In our experiments, we have empirically found that 15% to be a suitable threshold in this middle range representing the vibration signal arrivals.

4.3.2. Non-isotropic multilateration and component-based location averaging

Our non-isotropic multilateration formulation, which is able to consider various propagation velocities in different directions, has two main steps: (1) the simulation step and (2) the filtering step. The objective of the simulation step is to find the possible TDoA ranges caused by a footstep. To this end, we first define a Possible Location Set (PLS) for the footstep (e.g., inside the boundary of the room). Then, we estimate the sensor-footstep distances for various locations inside the PLS. Finally, we estimate the TDoAs for various sensor pairs for a given wave propagation velocity array. This wave propagation velocity array contains the velocities between the footstep location and each one of the sensors and is achieved from Section 4.2.4. Therefore, the simulation step results in a Possible TDoA Set (PTS) for locations in PLS. The objective of the filtering step is to find the locations in the PLS which result in TDoAs similar to the measured TDoAs. Specifically, we first find the actual TDoA values for various sensor pairs (as discussed in Section 4.3.1) and then, filter the TDoAs in PTS which are similar to the actual TDoAs. Finally, we find the locations in PLS which correspond to the remaining TDoAs in PTS. The detailed steps of our non-isotropic multilateration is presented in Algorithm 1. Finally, to improve the accuracy and robustness of our location estimation approach, we average multiple location estimations from the scale components selected in Section 4.2.3.

Algorithm 1. The non-isotropic multilateration approach

1: Define the Possible Location Set (PLS) of the Footstep ▷Simulation Step ↓
2: **for** PLS_i in PLS **do**
3: **for** S_j in sensor-locations **do**
4: $d_{ij} = \|X_i - S_j\|_2$
5: $ToA_j = d_{ij} \,/\, v_j$
6: **end for**
7: $TDoA_i = ToA - ToA[1]$
8: Possible TDoA Set (PTS) $\leftarrow$ $TDoA_i$
9: **end for**

```
10: ————————————————————————————————————
11: Estimate the actual pairwise TDoAs (AT)  ▷Filtering Step ↓
12: Define Required-Number-of-Estimations (RNE), init-thresh, update-thresh;
13: thresh ← init-thresh
14: while number-of-estimations  < RNE do
15:   forPTS_i in PTS do
16:     if PTS_i + thresh < AT < PTS_i + thresh then
17:       ELS ← PLS_i
18:     end if
19:   end for
20:   number-of-estimations ← number of elements in ELS
21:   thresh += update-thresh
22: end while
23: Estimated Location ← mean(ELS)
```

5. Obstruction-invariant occupant localization evaluation

To understand the performance of our obstruction-invariant occupant localization approach, we conducted a set of experiments with a human participant in real-world structures. We first introduce the experimental setup in Section 5.1. Then, we validate the performance of our obstruction-invariant occupant localization approach. This evaluation consists of the general performance as well as the performance of different modules of the approach (in Sections 5.2–5.6). Finally, we evaluate the sensitivity of our approach to the changes in the footstep-sensor distance, mass level, scale components, and structure (in Sections 5.7–5.10). Table 1 provides a summary of the different evaluation sections and objectives. It is necessary to mention that the main objective of this evaluation is to validate our sensing system for occupant localization in obstructive indoor settings and its different modules using real-world experiments. Rigorous evaluation of the inverse vibration problem and its theory is part of our future work, which will be discussed in Section 6.

5.1. Experimental setup

To evaluate our approach, we have utilized a sensing system which measures the floor vibration via a geophone. Geophone is a sensor which converts the vertical velocity of the floor to Voltage [41]. Fig. 6 shows a sample sensing node. The collected signals are amplified approximately 200-2000X. After amplification and depending on the structure type and footstep strike energy, the effective sensing range of our system for footstep detection is up to 20 meters in diameter. Amplified signals are then digitized and transferred to a server using a 24-bit A/D converter. To ensure enough time resolution for accurate TDoA estimation, we have chosen sampling frequency of 25 kHz. (see Fig. 7).

Sensing Configuration: For the experiments, the subject walks in two different structures to show that our approach is robust in across structures. The structures include a non-carpeted concrete floor on the ground level of a campus building in Carnegie Mellon University and a non-carpeted an elevated wood framed mock floor. The difference between the natural frequencies of these structures (i.e., 23.83 and 29.5 Hz, respectively) make them suitable to show the robustness of our approach over various structures. Fig. 8 shows the two experimental locations. To mimic the effect of the obstruction mass, we have used a plastic bin filled with sand. Based on the amount of the sand, we have achieved different levels of additional mass between 0 and 60 kg. For each of the 13 mass levels considered, we have collected 5 traces of four steps from each structure. To focus on the effect of the obstruction, these four step locations are chosen inside the polygon created by the sensors. The reason is that for steps outside this polygon, multilateration performance decreases quickly and hence the

Table 1
Evaluation objectives in different sections.

Section	Evaluation Objective
5.1	The sensing configuration
5.2	The overall footstep localization accuracy
5.3	The mass estimation performance
5.4	The scale component selection effect
5.5	The obstructed wave propagation velocity estimation performance
5.6	The non-isotropic multilateration performance
5.7	Sensitivity to different footstep-sensor distances
5.8	Sensitivity to changes in the obstruction mass
5.9	Sensitivity across different scale components
5.10	Sensitivity across different structures

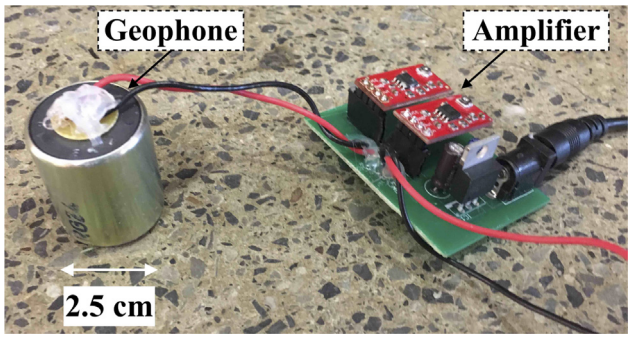

Fig. 6. The sensing node. These geophone sensors measures the vertical velocity of floor vibrations which is then amplified and transferred to a server for analysis.

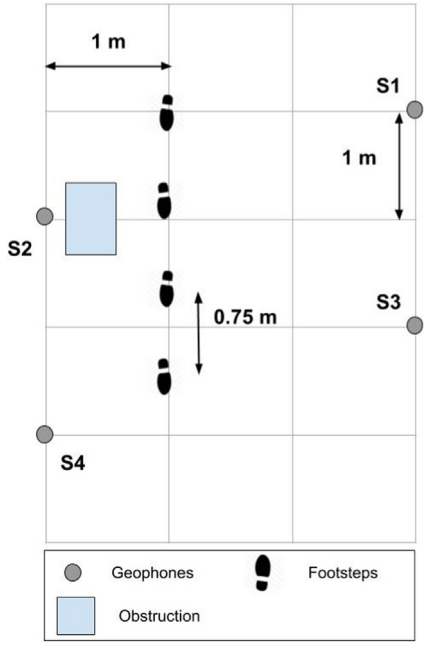

Fig. 7. The sensing configuration.

results become too uncertain to effectively and accurately study the effect of the obstruction [19]. In this paper, we focus on evaluating the effect of obstructions on the vibration waves and hence use one human subject. However, we have successfully localized multiple human subjects (one person walking at a time) in our prior work [19]. Therefore, we believe that our approach can be used across different subjects. As the main contribution of this paper is to show the potential of addressing the effect and challenges caused by the obstructions, we did not control the experiments in terms of the occupant velocity and asked the occupants to walk in a natural and comfortable way. Further, the subject wears flat-bottom footwear. To obtain the ground truth, we have taped the locations of the footsteps on the floor and asked the subjects to walk on these locations.

Unobstructed Velocity: Our obstruction characterization module aims to find the obstructed velocity as a ratio of the unobstructed velocity. This ensures that our approach is able to localize footsteps across various structures. To find the unobstructed velocity, in our prior work, we have introduced a multilateration solution approach which estimates the location and propagation velocity simultaneously [19]. However, the objective of this work is to study the obstruction effects and therefore, to reduce the uncertainties in estimating the propagation velocities, we calibrate for the velocity which results in the minimum localization error in a set of experiments with no obstruction [22].

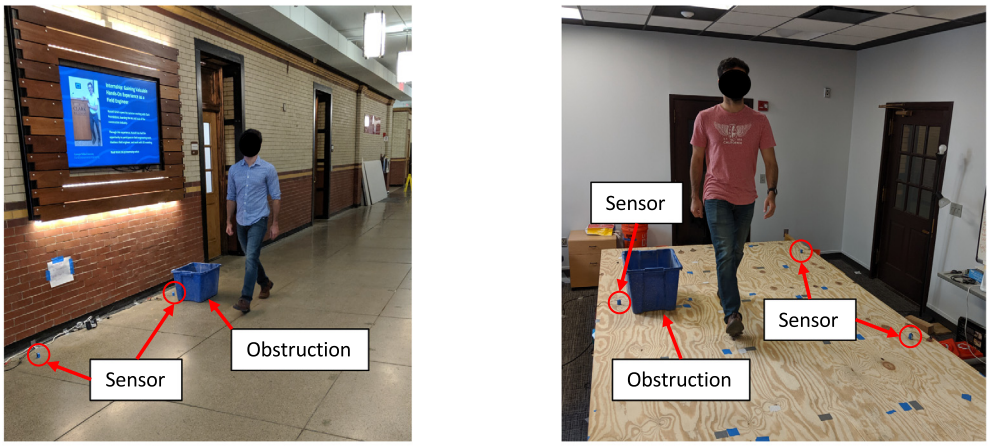

(a) CMU Porter Hall: Concrete Slab on Grade

(b) CMU Lab: Mock Wood Floor

Fig. 8. Experimental locations.

5.2. Overall footstep localization evaluation

To evaluate the performance of our obstruction-invariant occupant localization approach, we compare our localization errors with a baseline approach. The baseline approach (1) averages the estimations across all the scale components ("AllScale" approach), (2) does not account for the effect of the obstruction ("NoVelCorrect" approach), (3) utilizes a Nonlinear Least Square (NLS) ToA-based multilateration ("ToAMult" approach). Further, we compare our approach with the unobstructed case (i.e., there is no obstruction). The localization error metric is the Euclidean distance between the actual and estimated locations. As shown in Fig. 9, our approach results in 0.63 meters average error which is equivalent to 1.7X improvement over the baseline approach which has 1.07 meters error. Further, the unobstructed approach has 0.63 meters average error which is similar to our approach. These results show that our obstruction-invariant localization approach (1) successfully negates the effect of the obstruction and results in similar performance to the unobstructed approach and (2) outperforms the baseline approach. There are various ways to improve the localization accuracy. Some examples include adaptive scale component selection [19] and location tracking algorithms (e.g., Kalman filters [55]). However, such a task is out of the scope of this paper as the main contribution of this paper is to show the potential of addressing the effect and challenges caused by the obstructions. This will enable using sensors which do not have an unobstructed path between them (e.g., sensors in different rooms) and improve the sensing sparsity.

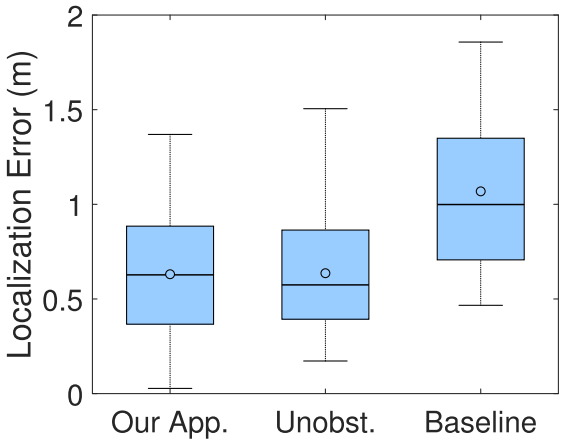

Fig. 9. The overall performance of our obstruction-invariant occupant localization approach. Our approach results in 0.63 meters average error which is (1) similar to the unobstructed case and (2) 1.7X improvement over the baseline approach which results in 1.97 meters error.

5.3. Mass estimation evaluation

In this section, we evaluate the performance of our mass estimation module. To this end, we first discuss the mass estimation performance and then study its sensitivity to the number of chosen features.

5.3.1. Mass estimation performance

As we discussed in Section 4.2.1, our approach predicts the mass through the ratios between the amplitude of the different frequency components of the vibration signals. To evaluate this approach, we compare the its results with a baseline approach which trains a linear regression model using all the components of the frequency representation of the vibration signals (instead of the ratios). As shown in Fig. 10a, in the first structure, our approach results in average mass estimation error of 12.7 kg, whereas the baseline approach results in average error of 29.4 kg. This is equivalent to 2.3X improvement in the performance. Moreover, our approach results in estimation standard deviation of 8 kg compared to 23 kg using the baseline approach (i.e., 2.9X improvement). In the second structure, as shown in Fig. 10b, our approach results in average mass estimation error of 3.6 kg which is 4X improvement over the baseline approach which result in 14.8 kg error. With regards to the standard deviation, our approach result in 3.9 kg compared to 14.6 kg using the baseline approach (i.e., 3.7X improvement in robustness). These results show that our mass estimation is both more accurate and robust compared to the baseline approach. In general, the results are better in the second structure. This is because the second structure is a wooden floor and has lower mass. Therefore, the effect of the additional mass is more significant and easier to quantify.

5.3.2. Mass estimation sensitivity to the number of chosen scales

An important factor for mass estimation performance is the number of chosen ratio features. As discussed in Section 4.2.1, we choose a subset of the ratio features for mass estimation to reduce (1) the chance of over-fitting and (2) the computational cost of the model training. To evaluate the sensitivity of our mass estimation approach to this factor, we have estimated the test error for the ratio feature subsets of various size, as shown in Fig. 11. Based on this figure, the mass estimation performance is robust and consistent when the size of the ratio feature subsets is less than 25. In this paper, we have chosen subset size of 4 for mass estimation to minimize the mass estimation error while reducing the computational cost.

5.4. Scale component selection evaluation

As discussed in Section 4.2.3, the existence of obstruction results in additional attenuation which reduces the Signal-to-Noise (SNR) ratio and hence the localization performance. To overcome this effect, our scale selection approach chooses a subset of scale components with high energies. We first evaluate how the scale selection affects the performance of our obstruction-invariant occupant localization approach (in Section 5.4.1). Then, we discuss the sensitivity of our approach to the number of chosen scale components in Section 5.4.2.

5.4.1. Scale component selection performance

To validate the effect of our scale selection approach, we compare our results with the AllScale approach which averages the location estimation across all the scales. In comparison, our approach averages the location estimation over two of the scale components with the highest energy. The rest of the localization procedure is similar for both of the considered approaches. As shown in Fig. 12, our scale selection approach results in 0.61 meters average localization error which is

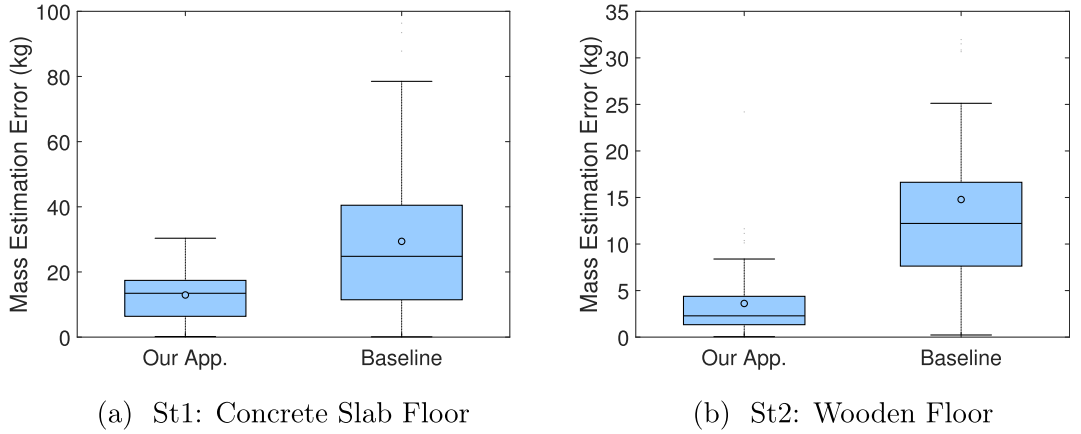

Fig. 10. The mass estimation evaluation. These figures show that our approach results in 12.7 and 3.6 kg error in mass estimation in the two structures. These are equivalent to 2.9X and 3.7X improvement over the baseline, respectively.

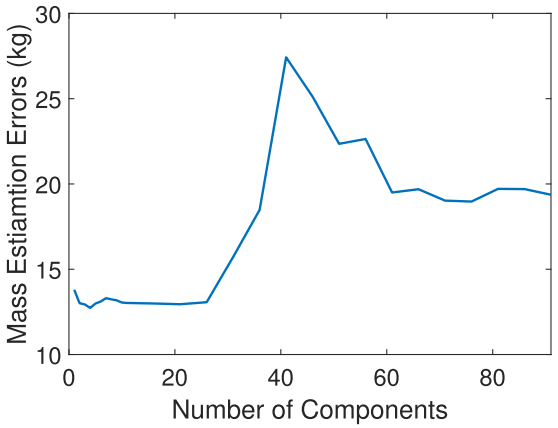

Fig. 11. Sensitivity of the mass estimation approach to the number of chosen ratio features. This figure shows that the mass estimation performance is robust and consistent when the size of the ratio feature subsets is less than 25.

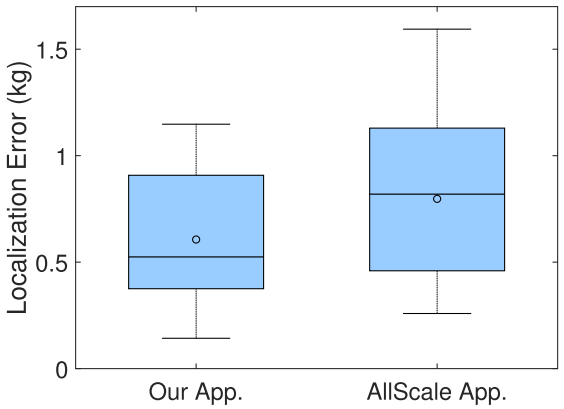

Fig. 12. Scale selection evaluation. Our scale selection approach results in 0.61 meters average localization error which is 1.3X improvement over the AllScale approach which results in 0.8 meters error.

1.3X improvement over the AllScale approach which results in 0.8 meters error. These results show that our scale selection approach chooses a suitable subset of scale components for occupant localization.

5.4.2. Localization performance sensitivity to the number of chosen scales

One of the factors that affects the performance of our obstruction-invariant localization approach is the number of the scale components. The trade-off is that: (1) choosing multiple scale components reduces the effect of erroneous and noisy location estimations (by averaging several estimations); however, (2) considering estimations from very low energy signals which mostly contain noise results in lower localization performance. To evaluate this factor, we have evaluated the localization performance across different number of scales. Fig. 13 shows this evaluation and the trade-off regarding the number of scale components. It can be seen that the localization performance is similar for cases with 2–20 scales. Therefore, in this paper, we empirically average over the location estimations of 2 scale components for footstep localization to ensure accurate localization while reducing the computational cost of the localization.

5.5. Obstructed wave propagation velocity estimation evaluation

In this section, we study the effect of the Obstructed Wave Propagation Velocity Estimation module. To this end, we compare our localization results with the NoVelCorrect approach which does not consider the effect of the obstruction on the wave propagation velocity. Similar to the previous sections, the rest of the localization procedure is similar between our approach and the NoVelCorrect approach. As shown in Fig. 14, our approach results in 0.61 meters average error which is equivalent to 1.2X improvement over the NoVelCorrect approach which results in 0.72 meters error. This improvement in performance shows that our wave propagation velocity estimation approach is effective in reducing the obstruction-induced propagation velocity changes.

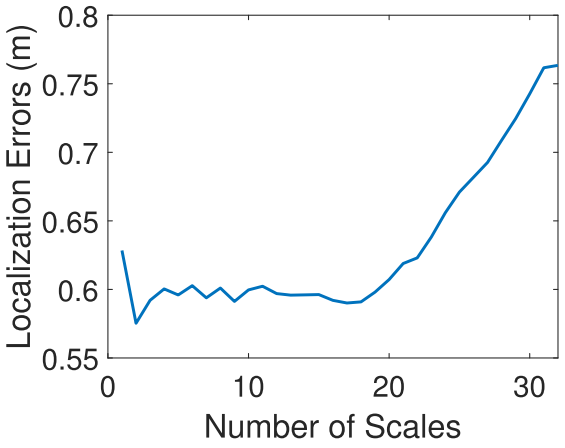

Fig. 13. The sensitivity of the approach to the number of chosen scales. Based on this figure, the localization performance is similar for cases with 2–20 scales.

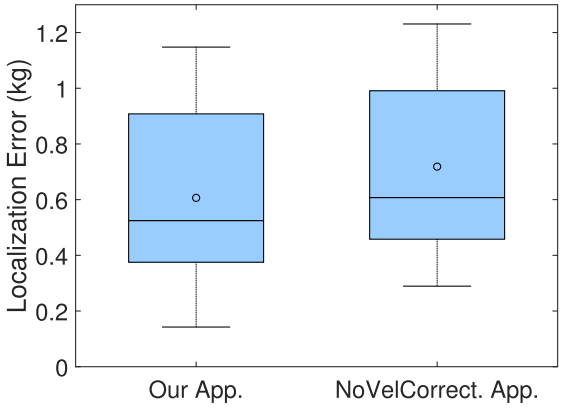

Fig. 14. Obstructed wave propagation velocity estimation evaluation. Our approach results in 0.61 meters average error which is equivalent to 1.2X improvement over the NoVelCorrect approach which results in 0.72 meters error.

5.6. Non-isotropic multilateration evaluation

Our non-isotropic multilateration approach enables occupant localization when there is different wave propagation velocities between the footstep and various sensors. To evaluate this approach, we compare our results with ToAMult which is a Nonlinear Least Square (NLS) based approach based on the Time of Arrival (ToA) of the vibration signal in the sensors. For the i^{th} sensor, ToAMult defines the following cost function:

$$C_i = \|x - p_i\|_2 - v_i(t_i - t_f) \tag{5}$$

where x is the location of the footstep, p_i is the location of the sensor, v_i is the propagation velocities between the footstep and the sensors, t_i is the vibration wave ToAs for the sensors, and finally t_f is the time that the footstep happens. There will be four equations for four sensors and the overall objective function is,

$$\min_{x,t_f} \sqrt{\sum_i C_i^2} \tag{6}$$

Knowing the wave propagation velocities, Eq. (6) can be solved for 3 unknowns: the 2-d footstep location (x) and the footstep occurrence time (t_f). Further, this formulations is a bounded nonlinear least-squares problem which can be solved using a trust region reflective algorithm [56].

Fig. 15 shows the results of this evaluation. Based on this figure, our approach results in average localization error of 0.61 meters error which is 2X improvement compared to the ToA-based approach (with average error of 1.23 meters meters). The reason behind this improvement is that adding the t_f as an unknown increases the dimension of the problem which in turn increases the likelihood of the NLS approach getting stuck in a local optimum. In comparison, our approach performs a grid

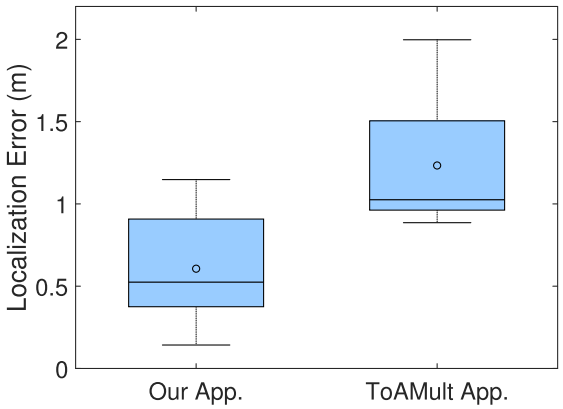

Fig. 15. Localization performance of the non-isotropic multilateration. This figure shows that our approach results in average localization error of 0.61 meters error which is 2X improvement compared to the ToA-based approach (with average error of 1.23 m).

search to find the globally optimum solution while keeping the online computational cost low by separating the offline simulation and online filtering step. The performance improvement shows that our non-isotropic multilateration approach is suitable for the real-life obstructed floors.

5.7. Localization performance sensitivity to changes in the footstep-sensor distances

Sensor-footstep distance is an important factor in the localization performance. To evaluate this factor, we find the localization errors for footsteps across different locations. Generally, the furthest sensor has the most effect on the localization error because (1) higher travelling distance between the sensor and the footstep means higher signal distortions and (2) the furthest signals generally have lower SNR which in turn results in lower localization performance. Therefore, to evaluate the effect of distance, the footstep-sensor distance for each footstep is found as the maximum of the Euclidean distances between the footstep and various sensors. Fig. 16 shows the results of this evaluation for our approach. As expected, the correlation coefficient of 0.71 shows that larger distances result in higher localization error. Specifically, our approach results in errors of 0.31–0.94 meters for the 2.4–3.4 maximum norm distance range.

5.8. Localization performance sensitivity to changes in the obstruction mass

Changing the obstruction mass results in changes in the wave propagation velocity which in turn, affects the localization performance. To evaluate this effect, we have conducted experiments with 12 levels of obstruction mass (each 5 kg between 0 and 60 kg). The localization results for these different added mass levels are presented in Fig. 17. Based on this figure, our approach outperforms the baseline approach for all the mass levels. Further, the improvements are generally more significant for cases with higher added mass. For example, when there is 5 kg of added mass, our approach outperforms the baseline by 0.25 meters. However, this number is increased to 0.38 meters when there is 60 kg of added mass. The reason is that the higher added mass cause more significant changes in the wave propagation velocity which, in turn, reduce the localization accuracy of the baseline approach. However, our approach considers this obstruction-induced velocity changes and therefore is less affected by the additional mass. This consistent improvement across all the mass levels shows that our approach efficiently negates the effect of the obstructions.

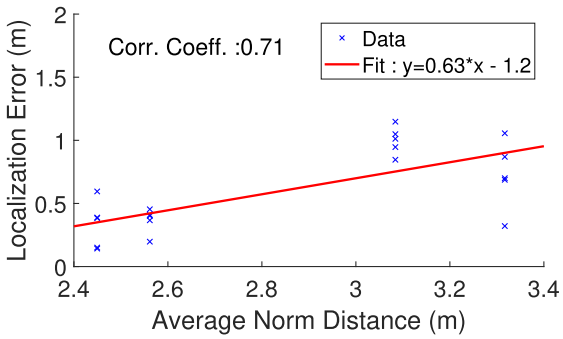

Fig. 16. Localization performance sensitivity to the footstep-sensor distance. As expected, larger distances result in higher localization error.

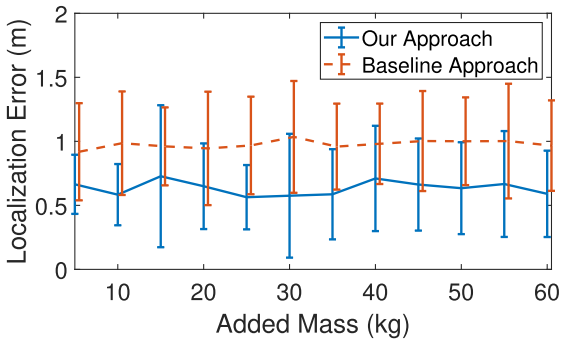

Fig. 17. The sensitivity of our obstruction-invariant occupant localization approach to the obstruction mass. Based on this figure, our approach outperforms the baseline approach for all the mass levels and therefore efficiently negates the effect of the obstructions.

5.9. Localization performance sensitivity to the scale components

In this section, we evaluate the improvement resulted from our obstruction-invariant occupant localization approach across various scales. The baseline approach (1) does not account for the obstruction masses and (2) utilizes the ToAMult approach discussed in Section 5.6. For this analysis, we have focused on the scale range of 25 to 300 which corresponds to 20–250 Hz for the Mexican hat wavelet. This range is decided by sensing specifications of the Geophone sensor, as discussed in Section 4.2.2. As shown in Fig. 18, our approach outperforms the baseline approach across all the scales. This shows that our obstruction-invariant occupant localization approach is more robust across all the scale components.

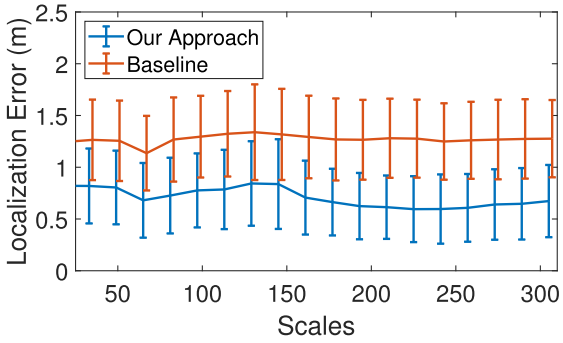

Fig. 18. Localization performance across various scales. This figure shows that our approach outperforms the baseline approach in all the scales.

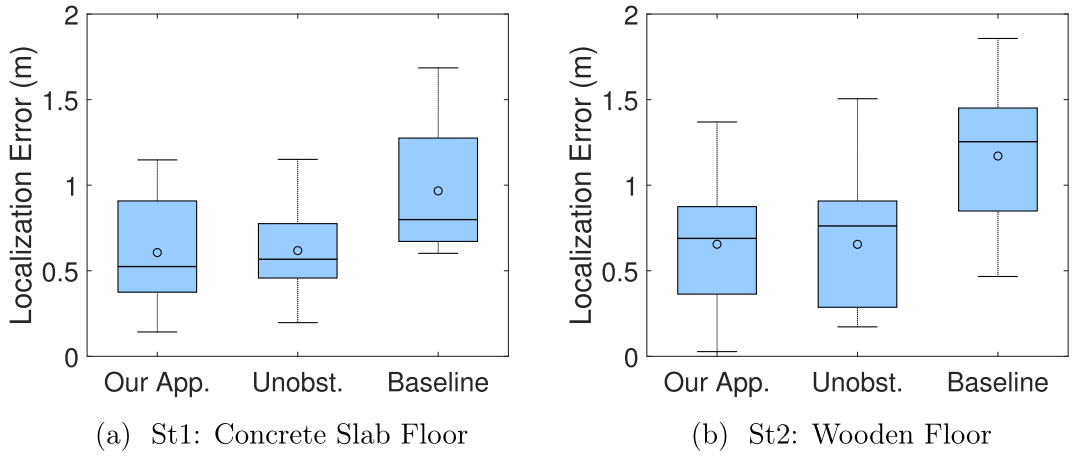

Fig. 19. Localization performance in different structures. In the first structure, our approach results in 0.61 m average localization error which is equivalent to 1.6X improvement over the baseline approach. In the second structure, our approach results in 0.65 meters which is equivalent to 1.8X improvements compared to the baseline approach. In both structures, our results are similar to the unobstructed cases.

5.10. Obstruction-invariant occupant localization evaluation across structures

By leveraging the lamb wave propagation characteristics, our obstruction-invariant occupant localization is robust across various structures. To evaluate this robustness, we have performed experiments in two different structures. For each structure, we have compared the performance of our approach with the baseline and the unobstructed approach. Fig. 19a shows the results for the first structure which is a non-carpeted concrete slab on the ground level of a campus building in Carnegie Mellon University in Pittsburgh, PA. This figure shows that our approach results in 0.61 meters average localization error which is equivalent to 1.6X improvement over the baseline approach which results in 0.97 meters average error. Further, in this structure, our approach has comparable results with the unobstructed approach which results in 0.62 meters average error. Fig. 19b show the results for the second structure which is a non-carpeted elevated mock wooden floor. In this structure, our approach results in 0.65 meters which is equivalent to 1.8X improvements compared to the baseline approach average localization error which is 1.17 meters. Despite the slightly higher localization errors (which is possibly caused by noisy nature of wooden floor vibrations [19]), our approach results in comparable localization performance to the unobstructed approach with 0.65 meters average error. These results shows that our obstruction-invariant occupant localization approach is robust to the changes in the structure which in turn, shows that it is practical in real-life applications.

6. Future work and discussion

As discussed in Section 1, the main objective of this paper is to introduce a non-intrusive sensing system for occupant localization in obstructive indoor settings. With respect to the run-time of our approach, in MATLAB 2019a, localizing one footstep using two scale components and 3 inches resolution takes approximately 0.16 s using a Surface book 2 with 8 Gb Ram and 2.7 GHz Intel Core i7-8650U @1.9 GHz. Considering that the time between footsteps is generally higher than 0.5 s, this localization time is sufficient for our applications. In a real-world scenario, we expect the data to be sent to a cloud server. Using a cloud server would significantly decrease the processing time and guarantee real-time operation.

For our future work, we aim to study the following factors.

- As discussed before, the assumption of infinite thin plate is a reasonable approximation for localization purposes when the first arrival is the most important part of the vibration wave signal. However, in other applications (e.g., occupant detection and identification), the effect of reflection might be more important. Therefore, we plan to relax the assumption of infinite plate and explore the effect of the boundary conditions in our future work.
- In this paper, we have focused on characterizing the effect of mass because we have observed that it is one of the most important factors affecting the wave propagation velocity in our preliminary experiments. We plan to characterize other factors such as footstep-sensor distance and the obstruction area and shape in future work.
- In this work, we have assumed that there is only one obstruction in the path of the wave. However, in real-life applications, there might be multiple sources of obstruction on the path of the vibration wave. As part of the future work, we plan to study the effect of multiple obstructions on the path of the wave with different sensor-obstruction and footstep-obstruction distances.
- As mentioned in Section 4.3.1, we have used an energy-based approach with 15% threshold for estimating the TDoAs. However, this threshold might be structure-dependent. Therefore, as part of our future work, we plan to study its relationship to the threshold which results in the best localization performance with the structural characteristics.

7. Conclusion

In this paper, we presented an obstruction-invariant occupant localization approach using footstep-induced floor vibrations. Conventional vibration-based occupant localization approaches map the Time Differences of Arrivals (TDoA) between multiple sensors pairs to the footstep location by assuming similar wave propagation velocities between the footstep and the sensors. This assumption, although true in open spaces, does not always hold in real-life situations with various types of obstruction (walls, furniture, etc.). These obstructions add to the mass of the floor on the path of the vibration waves which in turn affect the wave propagation velocity and reduces the occupant localization performance. To overcome the obstruction effect, we characterize (1) the frequency-dependent attenuation rate of the footstep-induced vibrations to find the existence and mass of the obstruction and (2) the mass-velocity relationship based on the lamb wave properties to estimate the wave propagation velocities between the footstep and various sensors knowing the obstruction mass. Finally, we introduce a non-isotropic multilateration approach to leverage these propagation velocities and the TDoA values across the signals for step-level occupant localization. Our approach resulted in a 0.61 meters average location estimation error, which corresponds to a 1.6X improvement compared to the baseline that does not account for obstructions. Further, our approach results in the same localization performance compared to the case with no obstruction which shows that it effectively negates the effect of the obstruction. By providing a sparse and non-intrusive occupant localization approach which works well in obstructed indoor areas, our system can significantly reduce cost for occupant sensing in future smart building applications.

CRediT authorship contribution statement

Mostafa Mirshekari: Conceptualization, Data curation, Formal analysis, Investigation, Methodology, Software, Validation, Visualization. **Jonathon Fagert:** Conceptualization, Data curation, Writing - original draft, Writing - review & editing. **Shijia Pan:** Conceptualization, Data curation, Writing - review & editing. **Pei Zhang:** Conceptualization, Data curation, Writing - review & editing, Funding acquisition, Project administration, Resources, Supervision. **Hae Young Noh:** Conceptualization, Data curation, Writing - review & editing, Funding acquisition, Project administration, Resources, Supervision.

Declaration of Competing Interest

The authors declare that they have no known competing financial interests or personal relationships that could have appeared to influence the work reported in this paper.

Acknowledgments

This research was partially supported by NSF (CMMI-2026699), Google, Intel, and Highmark.

References

[1] W.P. Cully, S.L. Cotton, W.G. Scanlon, J. McQuiston, Localization algorithm performance in ultra low power active rfid based patient tracking, in, in: 2011 IEEE 22nd International Symposium on Personal Indoor and Mobile Radio Communications (PIMRC), IEEE, 2011, pp. 2158–2162.
[2] W.P. Cully, S.L. Cotton, W.G. Scanlon, Empirical performance of rssi-based monte carlo localisation for active rfid patient tracking systems, Int. J. Wireless Inf. Networks 19 (3) (2012) 173–184.
[3] H. Visser, Gait and balance in senile dementia of alzheimer's type, Age Ageing 12 (4) (1983) 296–301.
[4] T. Oberg, A. Karsznia, K. Oberg, Basic gait parameters: reference data for normal subjects, 10–79 years of age, J. Rehabil. Res. Develop. 30 (2) (1993) 210.
[5] J. Fagert, M. Mirshekari, S. Pan, P. Zhang, H.Y. Noh, Characterizing left-right gait balance using footstep-induced structural vibrations, in: Sensors and Smart Structures Technologies for Civil, Mechanical, and Aerospace Systems 2017, Vol. 10168, International Society for Optics and Photonics, 2017, p. 1016819.
[6] S. Drira, Y. Reuland, S.G. Pai, H.Y. Noh, I.F. Smith, Model-based occupant tracking using slab-vibration measurements, Front. Built Environ. 5 (2019) 63.
[7] G. Diraco, A. Leone, P. Siciliano, People occupancy detection and profiling with 3d depth sensors for building energy management, Energy Build. 92 (2015) 246–266.
[8] C.M. Stoppel, F. Leite, Integrating probabilistic methods for describing occupant presence with building energy simulation models, Energy Build. 68 (2014) 99–107.
[9] C. Wang, X. Wang, Z. Long, J. Yuan, Y. Qian, J. Li, Estimation of temporal gait parameters using a wearable microphone-sensor-based system, Sensors 16 (12) (2016) 2167.
[10] P. Lazik, N. Rajagopal, O. Shih, B. Sinopoli, A. Rowe, Alps: A bluetooth and ultrasound platform for mapping and localization, in: Proceedings of the 13th ACM Conference on Embedded Networked Sensor Systems, ACM, 2015, pp. 73–84.
[11] E. Martin, O. Vinyals, G. Friedland, R. Bajcsy, Precise indoor localization using smart phones, in: Proceedings of the International Conference on Multimedia, ACM, 2010, pp. 787–790.
[12] J.T. Biehl, M. Cooper, G. Filby, S. Kratz, Loco: a ready-to-deploy framework for efficient room localization using wi-fi, in: Proceedings of the 2014 ACM International Joint Conference on Pervasive and Ubiquitous Computing, ACM, 2014, pp. 183–187.
[13] A.S. Paul, E.A. Wan, F. Adenwala, E. Schafermeyer, N. Preiser, J. Kaye, P.G. Jacobs, Mobilerf: a robust device-free tracking system based on a hybrid neural network hmm classifier, in: Proceedings of the 2014 ACM International Joint Conference on Pervasive and Ubiquitous Computing, ACM, 2014, pp. 159–170.
[14] Y. Li, X. Jing, H. Lv, J. Wang, Analysis of characteristics of two close stationary human targets detected by impulse radio uwb radar, Progr. Electromagn. Res. 126 (2012) 429–447.
[15] A. Purohit, Z. Sun, S. Pan, P. Zhang, Sugartrail: Indoor navigation in retail environments without surveys and maps, in: 2013 10th Annual IEEE Communications Society Conference on Sensor, Mesh and Ad Hoc Communications and Networks (SECON), IEEE, 2013, pp. 300–308.
[16] D. Savio, T. Ludwig, Smart carpet: A footstep tracking interface, in: 21st International Conference on Advanced Information Networking and Applications Workshops, 2007, AINAW'07, vol. 2, IEEE, 2007, pp. 754–760.
[17] M. Andries, O. Simonin, F. Charpillet, Localization of humans, objects, and robots interacting on load-sensing floors, IEEE Sens. J. 16 (4) (2016) 1026–1037.
[18] T. Murakita, T. Ikeda, H. Ishiguro, Human tracking using floor sensors based on the markov chain monte carlo method, in: Proceedings of the 17th International Conference on Pattern Recognition, 2004. ICPR 2004, vol. 4, IEEE, 2004, pp. 917–920.
[19] M. Mirshekari, S. Pan, J. Fagert, E.M. Schooler, P. Zhang, H.Y. Noh, Occupant localization using footstep-induced structural vibration, Mech. Syst. Signal Process. 112 (2018) 77–97.
[20] J. Achenbach, Wave Propagation in Elastic Solids, vol. 16, Elsevier, 2012.
[21] J.D. Poston, R.M. Buehrer, P.A. Tarazaga, Indoor footstep localization from structural dynamics instrumentation, Mech. Syst. Signal Process. 88 (2017) 224–239.
[22] M. Mirshekari, S. Pan, P. Zhang, H.Y. Noh, Characterizing wave propagation to improve indoor step-level person localization using floor vibration, in: Sensors and Smart Structures Technologies for Civil, Mechanical, and Aerospace Systems 2016, vol. 9803, International Society for Optics and Photonics, 2016, p. 980305.
[23] A. Pakhomov, A. Sicignano, M. Sandy, E.T. Goldburt, Single-and three-axis geophone: footstep detection with bearing estimation, localization, and tracking, in: Unattended Ground Sensor Technologies and Applications V, Vol. 5090, International Society for Optics and Photonics, 2003, pp. 155–161.
[24] J. Schloemann, V.S. Malladi, A.G. Woolard, J.M. Hamilton, R.M. Buehrer, P.A. Tarazaga, Vibration event localization in an instrumented building, Experimental Techniques, Rotating Machinery, and Acoustics, vol. 8, Springer, 2015, pp. 265–271.
[25] M. Setareh, R.D. Hanson, Tuned mass dampers to control floor vibration from humans, J. Struct. Eng. 118 (3) (1992) 741–762.
[26] J.-S. Hwang, H. Kim, D.-H. Moon, H.-G. Park, Control of floor vibration and noise using multiple tuned mass dampers, Noise Control Eng. J. 59 (6) (2011) 652–659.
[27] A.C. Webster, R. Vaicaitis, Application of tuned mass dampers to control vibrations of composite floor systems, Eng. J. Am. Inst. Steel Construct. 29 (3) (1992) 116–124.
[28] M. Setareh, J.K. Ritchey, A.J. Baxter, T.M. Murray, Pendulum tuned mass dampers for floor vibration control, J. Perform. Construct. Fac. 20 (1) (2006) 64–73.

[29] X. Yan, R. Zhu, G. Huang, F. Yuan, Focusing flexural lamb waves by designing elastic metamaterials bonded on a plate, in: Health Monitoring of Structural and Biological Systems 2013, Vol. 8695, International Society for Optics and Photonics, 2013, p. 86952P.
[30] X. Yan, R. Zhu, G. Huang, F.-G. Yuan, Focusing guided waves using surface bonded elastic metamaterials, Appl. Phys. Lett. 103 (12) (2013) 121901.
[31] B. Schwarz, A. Bauer, D. Gajewski, Passive seismic source localization via common-reflection-surface attributes, Studia geophysica et geodaetica 60 (3) (2016) 531–546.
[32] S. Asgari, J.Z. Stafsudd, R.E. Hudson, K. Yao, E. Taciroglu, Moving source localization using seismic signal processing, J. Sound Vib. 335 (2015) 384–396.
[33] U. Levy, E. Hemo, Robust source localization using decision-directed algorithm and confidence weights in unattended ground sensors system, in: 2012 IEEE International Conference on Multisensor Fusion and Integration for Intelligent Systems (MFI), IEEE, 2012, pp. 395–400.
[34] A.G. Woolard, V.S. Malladi, P.A. Tarazaga, et al., Classification of event location using matched filters via on-floor accelerometers, in: Sensors and Smart Structures Technologies for Civil, Mechanical, and Aerospace Systems 2017, vol. 10168, International Society for Optics and Photonics, 2017, p. 101681A.
[35] R. Bahroun, O. Michel, F. Frassati, M. Carmona, J.-L. Lacoume, New algorithm for footstep localization using seismic sensors in an indoor environment, J. Sound Vib. 333 (3) (2014) 1046–1066.
[36] Y. Reuland, S.G. Pai, S. Drira, I.F. Smith, Vibration-based occupant detection using a multiple-model approach, Dynamics of Civil Structures, vol. 2, Springer, 2017, pp. 49–56.
[37] I.A. Viktorov, Rayleigh and Lamb Waves: Physical Theory and Applications, Plenum Press, 1970.
[38] H. Kasama, M. Takemoto, K. Ono, Attenuation measurement of laser excited so-lamb wave by the wavelet transform and porosity estimation in superplastic al-mg plate, J. JSNDI 49 (4) (2000) 269–276.
[39] S. Mustapha, L. Ye, Non-destructive evaluation (nde) of composites: assessing debonding in sandwich panels using guided waves, in: Non-Destructive Evaluation (NDE) of Polymer Matrix Composites, Elsevier, 2013, pp. 238–278.
[40] H. Lamb, On waves in an elastic plate, Proc. Roy. Soc. London. Ser. A, Contain. Pap. Math. Phys. Char. 93 (648) (1917) 114–128.
[41] I/O Sensor Nederland bv, SM-24 Geophone Element, p/N 1004117, 2006.
[42] S. Pan, S. Xu, M. Mirshekari, P. Zhang, H.Y. Noh, Collaboratively adaptive vibration sensing system for high-fidelity monitoring of structural responses induced by pedestrians, Front. Built Environ. 3 (2017) 28.
[43] M. Mirshekari, J. Fagert, A. Bonde, P. Zhang, H.Y. Noh, Human gait monitoring using footstep-induced floor vibrations across different structures, in, in: Proceedings of the 2018 ACM International Joint Conference and 2018 International Symposium on Pervasive and Ubiquitous Computing and Wearable Computers, ACM, 2018, pp. 1382–1391.
[44] M. Mirshekari, J. Fagert, S. Pan, P. Zhang, H.Y. Noh, Forthcoming. step-level occupant detection across different structures through footstep-induced floor vibration using model transfer, J. Eng. Mech. doi:https://doi.org/10.1061/(ASCE)EM.1943-7889.0001719.
[45] M. Mirshekari, P. Zhang, H.Y. Noh, Calibration-free footstep frequency estimation using structural vibration, Dynamics of Civil Structures, vol. 2, Springer, 2017, pp. 287–289.
[46] M. Frigo, S.G. Johnson, Fftw: An adaptive software architecture for the fft, Proceedings of the 1998 IEEE International Conference on Acoustics, Speech and Signal Processing, ICASSP'98 (Cat. No. 98CH36181), vol. 3, IEEE, 1998, pp. 1381–1384.
[47] G. Chandrashekar, F. Sahin, A survey on feature selection methods, Comput. Electric. Eng. 40 (1) (2014) 16–28.
[48] M. Mirshekari, P. Zhang, H.Y. Noh, Non-intrusive occupant localization using floor vibrations in dispersive structure, in, in: Proceedings of the 14th ACM Conference on Embedded Network Sensor Systems CD-ROM, ACM, 2016, pp. 378–379.
[49] P.S. Addison, The Illustrated Wavelet Transform Handbook: Introductory Theory and Applications in Science, Engineering, Medicine and Finance, CRC Press, 2002.
[50] M. Edwards, X. Xie, Footstep pressure signal analysis for human identification, in, in: 2014 7th International Conference on Biomedical Engineering and Informatics (BMEI), IEEE, 2014, pp. 307–312.
[51] M. Alaziz, Z. Jia, J. Liu, R. Howard, Y. Chen, Y. Zhang, Motion scale: A body motion monitoring system using bed-mounted wireless load cells, in: 2016 IEEE First International Conference on Connected Health: Applications, Systems and Engineering Technologies (CHASE), IEEE, 2016, pp. 183–192.
[52] S. Pan, M. Mirshekari, J. Fagert, C.G. Ramirez, A.J. Chung, C.C. Hu, J.P. Shen, P. Zhang, H.Y. Noh, Characterizing human activity induced impulse and slip-pulse excitations through structural vibration, J. Sound Vib. 414 (2018) 61–80.
[53] J.-M. Valin, F. Michaud, J. Rouat, D. Létourneau, Robust sound source localization using a microphone array on a mobile robot, Proceedings 2003 IEEE/RSJ International Conference on Intelligent Robots and Systems (IROS 2003)(Cat. No. 03CH37453), vol. 2, IEEE, 2003, pp. 1228–1233.
[54] J.A. Paradiso, C. King Leo, Tracking and characterizing knocks atop large interactive displays, Sensor Rev. 25 (2) (2005) 134–143.
[55] S. Alajlouni, P. Tarazaga, A passive energy-based method for footstep impact localization, using an underfloor accelerometer sensor network with kalman filtering, J. Vib. Control 26 (11–12) (2020) 941–951.
[56] A.R. Conn, N.I. Gould, P.L. Toint, Trust Region Methods, vol. 1, Siam, 2000.